

Star Formation Indicators and Line Equivalent Width in Ly Galaxies

Mark Dijkstra^{1?} and Eduard W. Steyaert²

¹Astronomy Department, Harvard University, 60 Garden Street, Cambridge, MA 02138, USA

²Smithsonian Astrophysical Observatory, 60 Garden Street, Cambridge, MA 02138, USA

22 February 2024

ABSTRACT

The equivalent width (EW) of the Ly α line is directly related to the ratio of star formation rates determined from Ly α flux and UV α flux density [$\text{SFR}(\text{Ly}\alpha)/\text{SFR}(\text{UV})$]. We use published data (in the literature EW and $\text{SFR}(\text{Ly}\alpha)/\text{SFR}(\text{UV})$ are treated as independent quantities) to show that the predicted relation holds for the vast majority of observed Ly α emitting galaxies (LAEs). We show that the relation between EW and $\text{SFR}(\text{Ly}\alpha)/\text{SFR}(\text{UV})$ applies irrespective of a galaxy's "true" underlying star formation rate, and that its only source of scatter is the variation in the spectral slope of the UV continuum between individual galaxies. The derived relation, when combined with the observed EW distribution, implies that the ratio $\text{SFR}(\text{UV})/\text{SFR}(\text{Ly}\alpha)$ is described well by a log-normal distribution with a standard deviation of $0.3-0.35$. This result is useful when modelling the statistical properties of LAEs. We further discuss why the relation between EW and $\text{SFR}(\text{Ly}\alpha)/\text{SFR}(\text{UV})$ may help identifying galaxies with unusual stellar populations.

Key words: galaxies: high redshift

1 INTRODUCTION

Lyman (hereafter Ly α) equivalent width represents a fundamental quantity in the study of Ly α emitting galaxies. The equivalent width (EW) of the Ly α line emitted by galaxies is a sensitive indicator of the initial mass function (IMF) or gas metallicity from which stars form (e.g. Schaerer 2002, 2003). The existence of large equivalent width (rest-frame EW $\gtrsim 240\text{\AA}$) Ly α emitters has led to speculation on whether population III formation from pristine gas may actually have been observed (Malhotra & Rhoads 2002; Jimenez & Haiman 2006; Dijkstra & Wyithe 2007). However, this interpretation depends sensitively on the details of radiative transfer through both the intergalactic medium (IGM, see e.g. Schaerer 2008, for a discussion), and the interstellar medium (ISM, e.g. Neufeld 1991; Hansen & Oh 2006; Finkelstein et al. 2008). It is safe to conclude that at present, no truly convincing candidates for population III galaxies exist. The search for large equivalent width Ly α emitters (and population III galaxy formation) is a key science driver for the observational community, while modelling Ly α radiative transfer in large EW emitters is a challenge for theorists.

The main goal of this paper is to draw attention to the fact that Ly α EW is frequently discussed inde-

pendently from the quantity $\text{SFR}(\text{Ly}\alpha)/\text{SFR}(\text{UV})$ (e.g. Ajiki et al. 2003; Fujita et al. 2003; Venemans et al. 2004; Shimasaku et al. 2006; Gronwall et al. 2007; Tapken et al. 2007; Pentericci et al. 2009). This quantity denotes the ratio of the star formation rates derived from the observed Ly α flux and rest-frame UV α flux density. One can consider the quantity $\text{SFR}(\text{Ly}\alpha)/\text{SFR}(\text{UV})$ as an "alternative" measurement of EW, because the quantities EW and $\text{SFR}(\text{Ly}\alpha)/\text{SFR}(\text{UV})$ are directly related (see x 2.1 of this paper, and e.g. Dijkstra & Wyithe 2007, Rauch et al. 2008, Dey et al. 2008, Nagamine et al. 2008, Nilsson et al. 2009). Since EW represents a fundamental property of Ly α emitting galaxies, a more detailed investigation of its relation to the ratio $\text{SFR}(\text{Ly}\alpha)/\text{SFR}(\text{UV})$ is warranted.

We derive the relation between EW and $\text{SFR}(\text{Ly}\alpha)/\text{SFR}(\text{UV})$, and compare with observations in x 2. We discuss the implications of our results in x 3. Throughout this paper we denote the rest frame equivalent width by REW, and the observed equivalent width by OEWS. The two are related by $\text{REW} = \text{OEWS}/(1+z)$. When we write "EW" this refers to both OEWS and REWS.

? E-mail: dijkstra@cfa.harvard.edu

2 THE CORRELATION BETWEEN EW AND $\text{SFR}(\text{Ly})/\text{SFR}(\text{UV})$

2.1 The basis of the Correlation

The star formation rate derived from the Ly line is obtained from the better-calibrated H star formation indicator given by $\text{SFR}(\text{H}) = 7.9 \times 10^{-42} L_{\text{H}} \text{ M yr}^{-1}$, where L_{H} is the H luminosity in erg s^{-1} (e.g. Kennicutt 1998). For case-B recombination the corresponding Ly luminosity of the source is $L_{\text{Ly}} = 8.7 L_{\text{H}}$, and thus $\text{SFR}(\text{Ly}) = 9.1 \times 10^{-43} L_{\text{Ly}} \text{ M yr}^{-1}$.

Similarly, the star formation rate obtained from the UV luminosity density is generally given by $\text{SFR}(\text{UV}) = 1.4 \times 10^{-28} L_{\text{UV}} \text{ M yr}^{-1}$ (Kennicutt 1998). L_{UV} is the UV luminosity density in $\text{erg s}^{-1} \text{ Hz}^{-1}$ measured at $\lambda_{\text{UV}} = 1400 \text{ \AA}$. To be consistent with published work we shall assume $\lambda_{\text{UV}} = 1400 \text{ \AA}$. Formally, the standard conversion applies when $\lambda_{\text{UV}} = 1500 - 2800 \text{ \AA}$ (e.g. Kennicutt 1998), and the assumed star formation calibrators may not be completely accurate. This only introduces a minor systematic uncertainty in the connection of UV flux density to an actual star formation rate, and our working assumption $\lambda_{\text{UV}} = 1400 \text{ \AA}$ does not affect our main conclusions at all.

For the star formation calibrators discussed above, the ratio $\text{SFR}(\text{Ly})/\text{SFR}(\text{UV})$ is

$$\frac{\text{SFR}(\text{Ly})}{\text{SFR}(\text{UV})} = \frac{9.1 \times 10^{-43} L_{\text{Ly}}}{1.4 \times 10^{-28} L_{\text{UV}}} \quad (1)$$

The Ly rest-frame equivalent width is defined as

$$\text{REW} = \frac{L_{\text{Ly}}}{L_{\text{UV}}} = \frac{L_{\text{Ly}}}{L_{\text{UV}}}; \quad (2)$$

with L_{UV} (L_{Ly}) the flux density in $\text{erg s}^{-1} \text{ \AA}^{-1}$ ($\text{erg s}^{-1} \text{ Hz}^{-1}$) of the continuum just redward of the Ly emission line, and $\lambda_{\text{Ly}} = 1216 \text{ \AA}$ ($\nu_{\text{Ly}} = 2.46 \times 10^{15} \text{ Hz}$) denotes the wavelength (frequency) of the Ly transition. We further used the identity $L = L_{\text{Ly}}$ to obtain the right hand side of Eq 2.

We combine Eq 1 and Eq 2 and find

$$\frac{\text{SFR}(\text{Ly})}{\text{SFR}(\text{UV})} = \frac{\text{REW}}{\text{REW}_c} \frac{L_{\text{UV}}}{L_{\text{UV}}}; \quad (3)$$

with $\text{REW}_c = \frac{1.4 \times 10^{-28} L_{\text{UV}}}{9.1 \times 10^{-43} L_{\text{Ly}}} = 76 \text{ \AA}$. The ratio of the continuum flux densities at $\lambda_{\text{UV}} = 1216 \text{ \AA}$ and $\lambda_{\text{UV}} = 1400 \text{ \AA}$ ($L_{\text{UV}} = L_{\text{UV}}$) depends on the slope of the continuum. This slope is usually denoted by the parameter $d \log L = d \log L_{\text{UV}} / d \log \lambda_{\text{UV}}$ (i.e. $L \propto \lambda_{\text{UV}}^{\alpha}$ and $L \propto \nu_{\text{UV}}^{-\beta}$). We rewrite Eq 3 as

$$\frac{\text{SFR}(\text{Ly})}{\text{SFR}(\text{UV})} = \left(\frac{\text{REW}}{\text{REW}_c} \right) \left(\frac{L_{\text{UV}}}{L_{\text{UV}}} \right)^{\alpha} C \left(\frac{\text{REW}}{\text{REW}_c} \right); \quad (4)$$

Eq 4 shows that the ratio $\text{SFR}(\text{Ly})/\text{SFR}(\text{UV})$ is determined uniquely by REW and α , because REW_c , L_{UV} , and λ_{UV} are constants. The precise choice¹ of star formation calibrator enters entirely through the value of REW_c , and thus

the slope of the correlation. Provided that the same star formation calibrators are applied consistently to an ensemble of galaxies, the actual star formation rates in these galaxies are irrelevant to the existence of the correlation.

Furthermore, any scatter in the correlation between REW and $\text{SFR}(\text{Ly})/\text{SFR}(\text{UV})$ enters entirely through scatter in L_{UV} . Emission line galaxies at $z \approx 5.7$ show that $0.1 < \alpha < 2.4$ for $> 90\%$ of the galaxies (Tapken et al. 2007). This is consistent with the median value $\alpha_{\text{med}} = 1.4$ for Ly emitting objects at $z \approx 3$ determined by e.g. Venemans et al. (2005). Thus, we conservatively adopt $\alpha = 1.2 \pm 1.2$, which translates to $C = 0.89^{+0.16}_{-0.14}$ for $\lambda_{\text{UV}} = 1400 \text{ \AA}$.

2.2 Processes that affect the Correlation

Obtaining L_{Ly} and L_{UV} from the measured quantities F_{Ly} (the Ly flux in $\text{erg s}^{-1} \text{ cm}^{-2}$), and f_{UV} (the UV continuum flux density in $\text{erg s}^{-1} \text{ cm}^{-2} \text{ Hz}^{-1}$) is non-trivial as it requires various "corrections" that account for the fact that only a fraction of all emitted UV and Ly photons are observed. None of these corrections are trivial:

(i) For example, the IGM is expected to be opaque (transparent) to photons that were emitted blueward (redward) of the Ly resonance. To first order, this implies that only 50% of the Ly photons are transmitted to the observer. However, peculiar velocities of intergalactic gas (e.g. Dijkstra et al. 2007; Iliev et al. 2008), and radiative transfer effects in the ISM of galaxies (e.g. Ahn et al. 2003; Verhamme et al. 2008) make this correction quite uncertain. The escape fraction of Ly photons from the ISM of galaxies is heavily regulated by the presence and distribution of dust, as well as H I gas kinematics (Kunth et al. 1998; Hayes et al. 2009; Ostriker et al. 2009; Atek et al. 2008). This can cause the Ly escape fraction to vary significantly between objects, or even between different sight-lines within the same object (Laursen et al. 2009).

(ii) Dust also affects the UV continuum. The spectral slope in the UV continuum correlates with the amount of dust extinction (e.g. Calzetti et al. 1994; Heckman et al. 1998). The UV continuum slope for unobscured star-forming galaxies, α_{int} , varies between 0 - 2.6 depending on the age, initial mass function, and the star formation history of a galaxy (see e.g. Figs 31 and 32 of Leitherer & Heckman 1995). Dust lowers the observed UV continuum slope to $\alpha = \alpha_{\text{int}} - \beta$, in which $\beta = 1.0 [E(B-V)/0.3]$ (Calzetti et al. 2000; where $E(B-V)$ denotes the colour excess).

Dust reduces the overall UV flux density by a factor of $\exp(-E(B-V)/0.1)$ (see e.g. Verhamme et al. 2008). The measured slope of the UV continuum and/or the colour excess $E(B-V)$ can constrain the amount of extinction of the UV continuum by dust. However these constraints are uncertain and depend on the intrinsic UV continuum and/or on the precise shape of the extinction curve (see e.g. Verhamme et al. 2008).

Combined these effects introduce large uncertainties in the conversion from observed Ly flux to intrinsic Ly luminosity, and from observed UV flux density to intrinsic UV luminosity density. Of course, corrections for dust and/or the IGM should affect the left and right hand side of Eq 4 equally. In practise however, the UV continuum at λ_{UV}

¹ For example, another conversion factor that is often found in the literature is $\text{SFR}(\text{UV}) = 1.25 \times 10^{-28} L_{\text{UV}} \text{ M yr}^{-1}$ (Madau et al. 1998). Additionally, the conversion from Ly luminosity to SFR depends on gas metallicity (see Schaerer 2003).

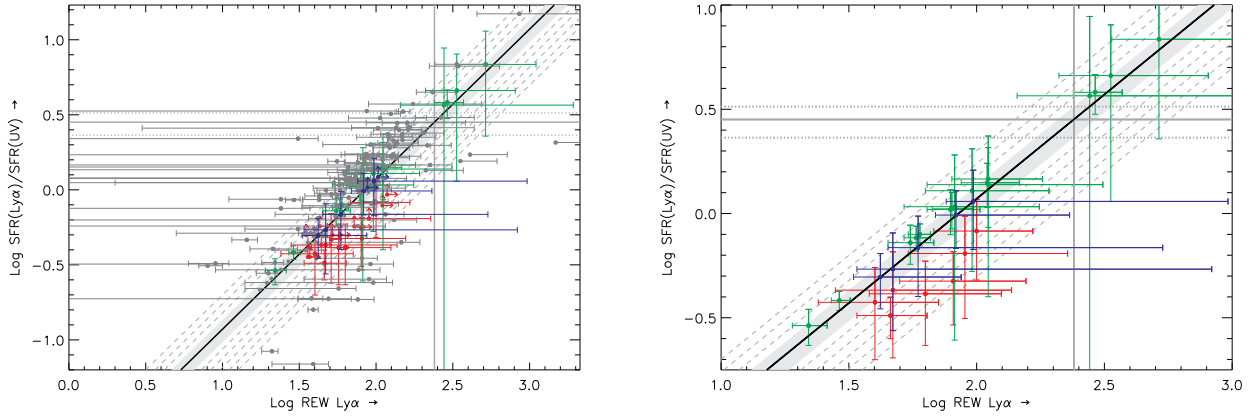


Figure 1. Comparison of the predicted correlation (Eq 4, solid line) and its 1 σ uncertainties (grey region) with published data (see text). Errorbars on all data points denote 1 σ uncertainties. Where errorbars are missing, the paper contained insufficient information to compute them. We show the relation $\text{SFR}(\text{Ly})/\text{SFR}(\text{UV}) = C(\text{REW}/\text{REW}_c)$ as the black solid line, where the grey shaded region denotes the 1 σ uncertainty in C . The grey dashed lines indicate the locations of galaxies that would have spectra with slopes $\beta = [-5; 5]$ with steps of 1. The vertical thick solid line denotes the maximum $\text{REW}_{\text{max}} = 240 \text{ \AA}$ that can be emitted by normal star-forming galaxies (e.g. Maltola & Rhoads 2002). Eq 4 converts this maximum REW into a maximum ratio $\text{SFR}(\text{Ly})/\text{SFR}(\text{UV})$, which is indicated with the horizontal thick solid grey line, and its 1 σ uncertainties are indicated with the horizontal thick dotted lines. The majority of data is consistent with the correlation given by Eq. 4. Statistically significant outliers correspond to galaxies with an unusual spectral slope of their continuum flux density. Right Panel: Same as left panel but focusing on the data points with published uncertainties on both REW and $\text{SFR}(\text{Ly})/\text{SFR}(\text{UV})$.

is often measured directly from the spectrum, while the continuum at $\lambda = \lambda_{\text{UV}}$ is determined from broadband imaging. Similarly, the Ly flux that enters the left and right hand side of Eq 4 may be obtained differently, e.g. from either the spectrum or from narrowband imaging. Clearly, this can introduce different systematic uncertainties to the measurements of $\text{SFR}(\text{Ly})/\text{SFR}(\text{UV})$ and EW. These uncertainties relate to, e.g. slit losses when taking spectra, dependence on aperture size and seeing for imaging, the precise filter curve of the narrowband filter (see e.g. Hayes & Ostriker 2006; Hayes et al. 2009, for extended discussions on complications that arise when determining λ and REW from broad and narrow band measurements).

Despite these complications, the quoted uncertainties on $\text{SFR}(\text{Ly})/\text{SFR}(\text{UV})$ and EW should reflect the systematic uncertainties, and we generally expect the data points to be consistent with Eq 4. Any statistically significant deviation implies that (i) some corrections are not applied consistently between the two measurements [e.g. the IGM is corrected for when determining the EW, but not when determining $\text{SFR}(\text{Ly})$], (ii) uncertainties in either EW or $\text{SFR}(\text{Ly})/\text{SFR}(\text{UV})$ have been underestimated, or (iii) the continuum of the galaxy has an unusual spectral slope.

The first two possibilities suggest that Eq 4 provides a convenient sanity check to whether the uncertainties in $\text{SFR}(\text{Ly})/\text{SFR}(\text{UV})$ and EW are estimated properly. The alternative, an unusual spectral slope is of great scientific interest. For example, objects that are dominated by nebular emission, such as galaxies that contain population III stars (Schaerer 2002) or cooling clouds (Dijkstra 2009), may be dominated by the two-photon continuum at $1216 \text{ \AA} < \lambda < 1600 \text{ \AA}$ (for which $\beta = 0$).

2.3 The C Correlation in Existing Data

We show the REW of LAEs versus the ratio of the SFRs for several surveys in Figure 1. The redshifts of the surveys range from $z = 3$ to 6.5 . The data are from Fujita et al. (2003), Taniguchi et al. (2005), Shimasaku et al. (2006), Ouchi et al. (2008) (grey data points), Ajiki et al. (2003, red points), Dawson et al. (2004, green points), and Venemans et al. (2004, blue points). We represent the data from Shimasaku et al. (2006) with two sets of points. We derive (i) the Ly flux from the narrowband filter, and the rest-frame UV flux density from the z-band, and (ii), the Ly flux from the spectrum, and the rest-frame UV flux density from the i-band. We use either the published values of REW and $\text{SFR}(\text{Ly})/\text{SFR}(\text{UV})$, or (when these are not readily available) computed their values from the available data. In theory, the correlation in Eq. 4 is independent of redshift. However, there are too few measurements available to observationally confirm this. The left panel of Figure 1 shows that the vast majority of galaxies are consistent with the relation given by Eq. 4 and appear to be normal star-forming galaxies.

The right panel of Figure 1 highlights the data points with published uncertainties in both REW and $\text{SFR}(\text{Ly})/\text{SFR}(\text{UV})$ from the left panel. These points illustrate more clearly that there are no significant outliers from the correlation given by Eq 4. We performed a least-squares linear fit to these data points of the form $\log \frac{\text{SFR}(\text{Ly})}{\text{SFR}(\text{UV})} = a + b \log \frac{\text{REW}}{\text{REW}_c}$, and obtained $a = -0.07 \pm 0.22$, and $b = 1.03 \pm 0.11$. This corresponds to $0.8 \pm 3\%$. Stronger constraints on β are not yet possible given the uncertainties in the data.

3 DISCUSSION AND CONCLUSIONS

We investigate the relation between REW and the ratio of star formation rates derived from Ly α flux, and rest-frame UV α density [SFR (Ly α)/SFR (UV)] (Eq 4). This relation derives directly from the definition of equivalent width and star formation rate conversion factors, and its only source of scatter is the variation in the slope of the UV continuum at Ly α $< <_{UV}$ between individual galaxies. The correlation exists regardless of the assumed star formation calibrators (which themselves depend on the assumed IMF and gas metallicity), or the true star formation rates of these galaxies.

Despite their fundamentally tight relation, Ly REW and SFR (Ly α)/SFR (UV) are often discussed as independent quantities. We investigate their correlation in existing data, and find the vast majority of galaxies to be consistent with the predicted relation (see Figs 1). The existence of the relation has interesting applications, which are discussed next.

3.1 An Empirically Constrained Ly α Based Star Formation Indicator

A SFR derived from the UV α density is likely more reliable than a SFR derived from Ly α flux. Ly α scatters through the ISM and IGM which makes it hard to determine the amount of extinction. Our relation can be used to derive a more accurate Ly α based star formation calibrator, if we require that (statistically) the Ly α derived SFR should be equal to the UV derived SFR. We introduce the constant M such that

$$\text{SFR}_M(\text{Ly } \alpha) = M \cdot \text{SFR}(\text{Ly } \alpha) / \text{SFR}(\text{UV}); \quad (5)$$

The constant M ensures that the SFR derived for a certain galaxy from its measured Ly α flux is equal to that derived from its UV α density. According to Eq 4 $M = [\text{C}(\text{REW} = \text{REW}_c)]^{-1}$; this implies that a galaxy with an unusually large REW has $M < 1$. Without this correction one would overestimate the SFR from the Ly α flux alone.

In the most general case, the probability $P(M) dM$ that M lies in the range M to $M + dM$ is given by (see Appendix A 1)

$$P(M) dM = dM N \int_1^\infty P(\lambda) P(\text{REW}_M) \frac{\text{REW}_M(\lambda)}{M} d\lambda; \quad (6)$$

with N the normalization factor which ensures that $\int_0^1 P(M) dM = 1$, and $\text{REW}_M(\lambda) = \text{REW}_c(M/\lambda)$. Furthermore, $P(\text{REW}) d\text{REW}$ denotes the probability that a LAE has an observed REW in the range REW to $\text{REW} + d\text{REW}/2$; $P(\lambda) d\lambda$ denotes the probability that a LAE has an observed λ in the range λ to $\lambda + d\lambda/2$.

Figure 2 shows the probability distribution $P(M)$ obtained from Eq 6 (black solid line). In this calculation we assume: (i) $P(\lambda)$ is a Gaussian with $\lambda = 1.2$, and $\sigma_\lambda = 0.9$. This choice ensures that 90% of the galaxies have $0.5 < M < 2.4$ (cf. Tapken et al. 2007); (ii) $P(\text{REW}) d\text{REW}$ is an exponential with a scale length of $\text{REW}_L = 76 \text{ \AA}$ (Gronwall et al. 2007), based on observed Ly α emitting galaxies at $z = 3.1$ with $\text{REW} > 20 \text{ \AA}$, i.e. $P(\text{REW}) d\text{REW} = \exp(-\text{REW}/\text{REW}_L)$ for $\text{REW} > \text{REW}_{\min} = 20 \text{ \AA}$, and $P(\text{REW}) = 0$ otherwise. In

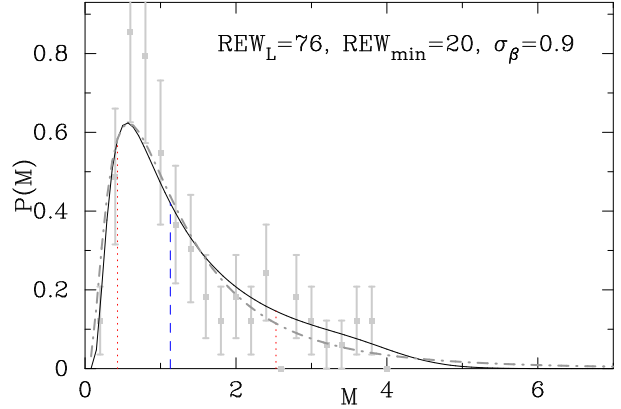


Figure 2. The black solid line shows the probability distribution for $M = \text{SFR}(\text{UV})/\text{SFR}(\text{Ly } \alpha)$ as given by Eq 4, in which $P(\text{REW})$ and $P(\lambda)$ are determined from the observations (see text). The red dotted lines mark the 68% confidence interval centered on the median $M = 1.13$ (indicated by the blue dashed line). We thus find that (68% of LAEs have $M = 1.1^{+1.4}_{-0.7}$). The data points denote the directly measured distribution of $\text{SFR}(\text{UV})/\text{SFR}(\text{Ly } \alpha)$ collected from the papers used in our analysis. The errorbars denote Poisson uncertainties in these data. The observed data distribution agrees well with our derived PDF. Furthermore, the derived PDF is reproduced quite well by a log-normal distribution which is indicated by the grey dot-dashed line, which is easily adopted when modeling statistical properties of LAEs.

Appendix A 2 we show that the precise shape of the distribution is not very sensitive to the assumed probability density functions (PDFs) of λ and REW.

Figure 2 shows that $P(M)$ peaks at $M = 0.6$. The function $P(M)$ is highly asymmetric and its median is $M = 1.13$, which is indicated as the blue dashed line. That is, $\text{SFR}(\text{Ly } \alpha) < 0.88 \text{ SFR}(\text{UV})$ for 50% of the galaxies (similarly, $\text{SFR}(\text{Ly } \alpha) < \text{SFR}(\text{UV})$ for 57% of the galaxies). The red dotted lines mark the 68% confidence interval centered on the median value. We therefore find that for 68% of LAEs $M = 1.1^{+1.4}_{-0.7}$. In other words, the Ly α derived SFR lies within a factor of 2.5 from the UV derived SFR for 68% of LAEs. Overplotted as the data points is the measured distribution of $\text{SFR}(\text{UV})/\text{SFR}(\text{Ly } \alpha)$ collected from the papers that were used in our analysis. The errorbars denote Poisson uncertainties. This observed distribution agrees quite well with our derived PDF. The grey dot-dashed line indicates a log-normal distribution

$$P(M) dM = \frac{1}{\sigma \sqrt{2\pi}} \exp\left[-\frac{1}{2\sigma^2} \left(\frac{\log M}{\sigma} + x\right)^2\right] \frac{dM}{M \ln 10}; \quad (7)$$

with $x = 0.04$ and $\sigma = 0.35$. This log-normal distribution provides a decent fit to the derived and observed distribution, and is easily adopted when modeling statistical properties of LAEs.

Ouchi et al. (2008) conclude that between $z = 3$ and $z = 6$ the observed REW PDF is consistent with no redshift evolution. This implies that our derived PDF for M also applies at redshifts greater than $z = 3$. On the other hand, the measured scale length of the exponential REW distribution at $z = 2.3$ is $\text{REW}_L = 48 \text{ \AA}$ (Nilsson et al. 2009), causing the PDF to broaden and shift to larger M (see Appendix A 2). Table 1 summarizes the redshift dependence of the pa-

Table 1. Fit Parameters for the log-normal PDF for P (log M)dM .

	x	
$z > 3$ ^a	0.04	0.35
$z < 3$	0.20	0.31

^a We assume that the REW -PDF, and hence the M -PDF, does not to evolve between $z = 3$ –6 (Ouchi et al. 2008). We take the observed $z = 3$ REW -PDF from Gronwall et al. (2007) for $z > 3$, and the observed $z = 2.3$ REW -PDF from Nilsson et al. (2009) for $z < 3$.

rameters describing the log-normal distribution for M . In both redshift bins the standard deviation of the log-normal distribution is very similar, with $\sigma = 0.3$ –0.35. The abrupt change of the value of x at $z = 3$ is clearly a crude approximation of the real redshift evolution of the M -PDF. We have chosen this parameterization because it corresponds to the simplest description that is consistent with existing data.

In theoretical work the inverse problem often arises in which a Ly luminosity must be obtained from a physical SFR. In such a case one may write $L_{\text{Ly}} = \frac{1.1 \cdot 10^{42} \text{ erg s}^{-1}}{M} \left(\frac{\text{SFR}}{M \text{ yr}^{-1}} \right)$ and adopt our PDF for M . This allows one to assign an empirically calibrated, variable Ly luminosity to galaxies of a given SFR. This prescription is clearly not perfect, because not all galaxies that are actively forming stars show a Ly emission line. For example, only 20–25% of Lyman Break galaxies (LBGs) at $z = 3$ have a Ly line with REW > 20% A and would classify as a LAE (e.g. Shapley et al. 2003), and the connection between LBGs and LAEs is not well understood. Nevertheless, our suggested prescription for assigning Ly luminosities to galaxies of a given SFR is more realistic than the often used one-to-one relation $L_{\text{Ly}} = 1.1 \cdot 10^{42} \text{ erg s}^{-1} \text{ SFR} (M \text{ yr}^{-1})$.

3.2 Outliers in the SFR (Ly)/SFR (UV)-REW Plane: Signposts for Unusual Galaxies?

"Normal" star forming galaxies can emit a maximum REW_{max} = 240 Å. Galaxies with REW > REW_{max} may signal the presence of a galaxy that contains population III stars (e.g. Malhotra & Rhoads 2002). Using Eq 4 this corresponds to $[SFR (Ly)/SFR (UV)]_{\text{max}} = 2.8^{+0.4}_{-0.5}$. The majority of observed galaxies that have quoted uncertainties on SFR (Ly)/SFR (UV) are consistent with this upper limit.

Objects where nebular emission dominates, such as galaxies containing population III stars (Schaerer 2002) or cooling clouds (Dijkstra 2009), may be dominated by the two-photon continuum at 1216 Å < λ < 1600 Å. This results in unusually negative values for β . These objects may have been identified in the spectrum itself, because deviations from the correlation are caused by unusual spectral slopes. However, reliable measurements of the continuum just redward of the Ly line and at $\lambda_{\text{UV}} = 1400$ Å provide a long baseline in wavelength, which may more clearly reveal the presence of a continuum dominated by two-photon emission. This suggests that outliers in the REW -SFR (Ly)/SFR (UV) plane may provide a more sensitive

probe to cooling clouds or primordial galaxies than the spectrum alone. That additional probe is important especially at high redshifts, where the IGM may transmit only a small fraction of the Ly emission by galaxies (Dijkstra et al. 2007). In this case even those star forming galaxies containing population III stars may have REW < REW_{max}. This strongly suggests that the determined REW alone is not enough to identify a population III galaxy.

Acknowledgements M.D. is supported by Harvard University funds. E.W. acknowledges the Smithsonian Institution for the support of his postdoctoral fellowship. We thank an anonymous referee for helpful, constructive comments that improved the content of this paper.

REFERENCES

- Ahn, S.-H., Lee, H.-W., & Lee, H.-M. 2003, MNRAS, 340, 863
 Ajiki, M., et al. 2003, AJ, 126, 2091
 Atek, H., Kunth, D., Hayes, M., Ostlin, G., & Mas-Hesse, J.M. 2008, A & A, 488, 491
 Calzetti, D., Kinney, A.L., & Storchi-Bergmann, T. 1994, ApJ, 429, 582
 Calzetti, D., Amus, L., Bohlin, R.C., Kinney, A.L., Koomneef, J., & Storchi-Bergmann, T. 2000, ApJ, 533, 682
 Dawson, S., et al. 2004, ApJ, 617, 707
 Dayal, P., Ferrara, A., & Gallerani, S. 2008, MNRAS, 389, 1683
 Dijkstra, M., Lidz, A., & Wyithe, J.S.B. 2007, MNRAS, 377, 1175
 Dijkstra, M., & Wyithe, J.S.B. 2007, MNRAS, 379, 1589
 Dijkstra, M. 2009, ApJ, 690, 82
 Finkelstein, S.L., Rhoads, J.E., Malhotra, S., Grogan, N., & Wang, J. 2008, ApJ, 678, 655
 Fujita, S.S., et al. 2003, AJ, 125, 13
 Gronwall, C., et al. 2007, ApJ, 667, 79
 Hansen, M., & Oh, S.P. 2006, MNRAS, 367, 979
 Hayes, M., Ostlin, G. 2006, A & A, 460, 681
 Hayes, M., Ostlin, G., Mas-Hesse, J.M., & Kunth, D. 2009, AJ, 138, 911
 Heckman, T.M., Robert, C., Leitherer, C., Garnett, D.R., & van der Rydt, F. 1998, ApJ, 503, 646
 Ilev, I.T., Shapiro, P.R., McDonald, P., Mellem, G., & Pen, U.-L. 2008, MNRAS, 391, 63
 Jimenez, R., & Haiman, Z. 2006, Nature, 440, 501
 Kennicutt, R.C., Jr. 1998, ARA & A, 36, 189
 Kunth, D., Mas-Hesse, J.M., Terlevich, E., Terlevich, R., Lequeux, J., & Fall, S.M. 1998, A & A, 334, 11
 Laursen, P., Razoumov, A.O., & Sommer-Larsen, J. 2009, ApJ, 696, 853
 Leitherer, C., & Heckman, T.M. 1995, ApJS, 96, 9
 Madau, P., Pozzetti, L., & Dickinson, M. 1998, ApJ, 498, 106
 Malhotra, S., & Rhoads, J.E. 2002, ApJL, 565, L71
 Nagamine, K., Ouchi, M., Springel, V., & Hemquist, L. 2008, arXiv:0802.0228
 Neufeld, D.A. 1991, ApJL, 370, L85
 Nilsson, K.K., Tapken, C., Moller, P., Freudling, W., Fynbo, J.P.U., Meisenheimer, K., Laursen, P., Ostlin, G. 2009, A & A, 498, 13

- Ostlin, G., Hayes, M., Kunth, D., Mas-Hesse, J. M., Leitherer, C., Petrosian, A., & Atek, H. 2009, *AJ*, 138, 923
- Ouchi, M., et al. 2008, *ApJS*, 176, 301
- Pentericci, L., Grazian, A., Fontana, A., Castellano, M., Giallongo, E., Salimbeni, S., & Santini, P. 2009, *A & A*, 494, 553
- Rauch, M., et al. 2008, *ApJ*, 681, 856
- Schaerer, D. 2002, *A & A*, 382, 28
- Schaerer, D. 2003, *A & A*, 397, 527
- Schaerer, D. 2008, *IAU Symposium*, 255, 66
- Shapley, A. E., Steidel, C. C., Pettini, M., & Adelberger, K. L. 2003, *ApJ*, 588, 65
- Shimasaku, K., et al. 2006, *PASJ*, 58, 313
- Tapken, C., Appenzeller, I., Noll, S., Richling, S., Heidt, J., Meikohn, E., & Mehlert, D. 2007, *A & A*, 467, 63
- Taniguchi, Y., et al. 2005, *PASJ*, 57, 165
- Venemans, B. P., et al. 2004, *A & A*, 424, L17
- Venemans, B. P., et al. 2005, *A & A*, 431, 793
- Verhamme, A., Schaerer, D., Atek, H., & Tapken, C. 2008, *A & A*, 491, 89

APPENDIX A: THE PROBABILITY DISTRIBUTION FUNCTION (PDF) FOR M

A.1 Derivation of $P(M)dM$

We employ the notation of probability theory, where the function $p(y|b)$ denotes the conditional probability density function (PDF) of y given b . The PDF for y is then given by $p(y) = \int p(y|b)p(b)db$, where $p(b)$ denotes the PDF for b . Similarly, we can write $p(y) = \int \int p(y|b;a)p(b)p(a)dbda$, where $p(y|b;a)$ denotes the conditional probability density function (PDF) of y given b and a , and where we assume that a and b are independent. We can thus write the probability $P(M)dM$ that M lies in the range M to $M+dM$ as

$$P(M)dM = dM \int_0^1 d \int_{\text{REW}_{\min}}^1 d\text{REW} \frac{P(M|j;\text{REW})}{P(\text{REW})P(j)}; \quad (\text{A1})$$

with REW_{\min} the minimum REW, and $P(M|j;\text{REW})$ the conditional PDF M given² j and REW .

Because we know that $\int_0^1 P(M|j;\text{REW})dM = 1$, and that for a given j and REW there is only one solution $M = [\mathcal{C}(\text{REW}=\text{REW}_c)]^{-1}$ (Eq 5), we write $P(M|j;\text{REW}) = \delta(M - [\mathcal{C}(\text{REW}=\text{REW}_c)]^{-1}) \delta(g(\text{REW}))$, where $\delta(x)$ denotes the standard Dirac-delta function. We eliminate the integral over REW by using the property of Dirac delta functions that $\delta(h(x)) = \frac{(\frac{x}{h'(x_0)})}{|h'(x_0)|}$, where x_0 denotes the (real) root of $h(x)$. If we denote the root of $g(\text{REW})$ with REW_M then $\delta(g(\text{REW}_M)) = \frac{M}{\text{REW}_M}$ and obtain Eq 6.

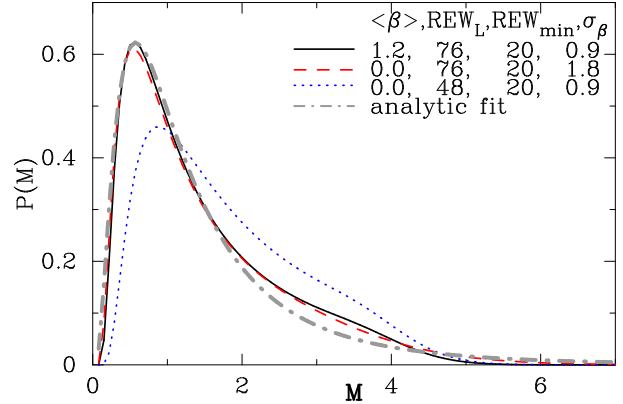


Figure A1. This Figure shows the dependence of $P(M)dM$ on various model parameters that describe the PDFs for j and REW , which include β , REW_L , REW_{\min} and σ_β . Each curve represents a calculation in which one of the model parameters – as indicated in the top right corner of the Figure – was varied.

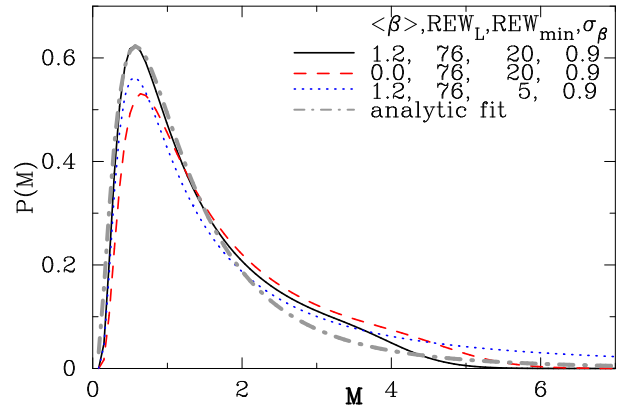


Figure A2. Same as Fig A1 but for model parameters indicated in the top right corner.

A.2 Dependence of $P(M)dM$ on Model Parameters

We investigate the dependence of $P(M)dM$ on various model parameters that describe the PDFs for j and REW , which include β , REW_L , REW_{\min} and σ_β . Figures A1 and A2 show the PDFs that we obtain when varying one of the model parameters as indicated in the top right corner of each Figure. For example, the red dashed line shows the PDF that we obtain for $\beta = 0.0$.

Figures A1 and A2 show that the PDF does not vary significantly when changing the parameters β , REW_L , and REW_{\min} . The PDF appears to be most sensitive to the scale length of exponential REW distribution. The value $\text{REW}_L = 48$ A corresponds to the scale length that was derived by Nilsson et al. (2009) for $z = 2.3$ LAEs. At these lower redshifts there is a lower fraction of large EW emitters, which pushes the M PDF to larger values.

² We assume that REW and j are independent variables. In the case that larger data sets demonstrate that this assumption is false, then one needs to replace $P(\text{REW})P(j)$ with $P(\text{REW}, j)$ in Eq A1.